**Research Article**

# Synthesis, Molecular Docking, and Cytotoxic Evaluation of Some Novel 1H-Pyrazole Derivatives from Pentoxifylline

JESSICA SHLIMOON HANNA[1]*, AYAD KAREEM KHAN[2], HAYDER JAFER ESSA[2]

[1]Department of Pharmacy, AL-Rasheed University College, Baghdad-Iraq.
[2]Department of Pharmaceutical Chemistry, College of Pharmacy, Mustansiriyah university, Baghdad-Iraq.
*Corresponding Author
Email: Jessicahanna@alrasheedcol.edu.iq.

## ABSTRACT

New Methylxanthine-based derivatives were designed synthesized and primarily screened for their cytotoxic activity against human A549 (lung) cancer cell line. Pentoxifylline (PTX) is a synthetic Methylxanthine derivative act as a nonselective phosphodiesterase inhibitor (PDEI). The new derivatives were designed by incorporating pyrazoline pharmacophore into Pentoxifylline. The Claisen-Schmidt condensation reaction were used to synthesize intermediates chalcone derivatives [1, 2, 3, 4, and 5]. The pyrazole derivatives [1a, and 1b] in the second step synthesized and all compounds were characterized by melting points, $R_f$ values, and confirmed by FT-IR and $^1$H-NMR spectroscopy. The computational methods done before synthesis including ADME studies were performed using the SwissADME server to predict the pharmacokinetics of the designed compounds. The results showed that all compounds expected passively and highly absorbed from The GIT. Besides, all synthesized compounds satisfied the Rule of five (RO5) except compound [1b]. The designed compounds checked for their selectivity towards EGFR by using GOLD suite software. All the designed compounds exhibit good binding energies with receptor active pocket and having promising activity with these proteins. The $IC_{50}$ values of the tested compounds exhibit that compounds [3, 4, 5, and 1b] have potent to moderate cytotoxic activity. Among them, the most potent was compound [5] with an $IC_{50}$ value of 11.44 µM compared to the standard drug Erlotinib with an $IC_{50}$ value of 25.23 µM. while the percentage of cell death was 81.21% for compound [5]; appear to be slightly lower than erlotinib with 82.40% of cell death.

**Keywords:** Pentoxifylline, Pyrazole, Docking Study, ADME Evaluation.

## INTRODUCTION

Generally, xanthine [1H-purine-2,6(3H,7H)-diones] and it is derivatives are purine based nitrogenous compounds, It is structure consist of pyrimidinedione fused with imidazole ring [1,2]. However, Xanthine derivatives are commonly known for their broad range of biological activities such as PDEs inhibitors, Alzheimer's disease, asthma, antidepressants, anxiolytics, cancer, diabetics, analgesic, parkinsonism, diuretic[2,3], and others.

Pentoxifylline is a synthetic Methylxanthine derivative. It is considered as a nonselective inhibitor of PDEs especially isozymes PDE3 and PDE4 that is primarily present in inflammatory cells[4,5]. It is the main indication is in the treatment of intermittent claudication primarily due to the role in reducing blood viscosity and increasing red blood cell deformability[5]. PTX activity and role in anticancer get significant attention nowadays[6]. PTX when used in combination with chemotherapy and radiotherapy showed synergistic activity with an increase in the effectiveness of therapy[7,8].

Chalcones on the other hand is an aromatic ketone that is present in many biological compounds as a central core and is related to the flavonoids family[9,10]. Chalcone derivatives possess a wide spectrum of biological activity such as antimicrobial, anti-inflammatory, antifungal [11], anticancer [12], antiviral activity [13], antimalarial[14], and others. Further, pyrazoles are considered as one of the substantial classes of five-membered heterocyclic compounds[15]. Pyrazole derivatives display anticancer activity due to their role in the inhibition of many targets[16] such as EGFR and HER-2 kinase inhibitors[17] VEGFR(18), CDKs[19], BRAF$^{V600F}$, Tubulin[20], and others. In this work, we report effective, simple, and convenient methods of chalcone and pyrazoline synthesis based on Methylxanthine pharmacophore. Then, evaluate their cytotoxic activity against the A549 (lung) cancer cell line.

## MATERIAL AND METHODS

Pentoxifylline was obtained from Sigma-Aldrich (USA), the aldehyde derivatives from Zhejiang Medicine Co. Ltd., Xinchang Pharmaceutical Factory (China). Remain chemical obtained from commercial sources and all used without extra purification. The TLC plate used was coated with aluminum [silica gel (60) F254], (Merck, Germany). Compounds were revealed upon irradiation with visible and UV light. Chromatograms were eluted by one solvent system: Methanol: chloroform (2:8). Melting point determined using Stuart electric melting point apparatus. By open-glass capillary tube method and reported without correction. Determination of infrared spectra by using Shimadzu-FT-IR infrared spectrometer, Performed by using KBr disc, in range (4000-400) cm$^{-1}$. The $^1$H-NMR

spectra were performed on instrument Inova-Varian 500 MHz spectrometer frequency. The chemical shift reported in (δ, ppm) and using DMSO-$d_6$ as a solvent for analyses. Docking studies performed using GOLD (Genetic Optimization for Ligand Docking) (v. 5.7.1), the software of Cambridge Crystallographic Data Center (CCDC). The crystal structure (3D) of the EGFR protein was got from the protein data bank (PDB).

### Chemical synthesis:

The synthesis of target compounds [1a, 1b] and their intermediates [1-5] was accomplished following procedures illustrated below in **Scheme (1)**
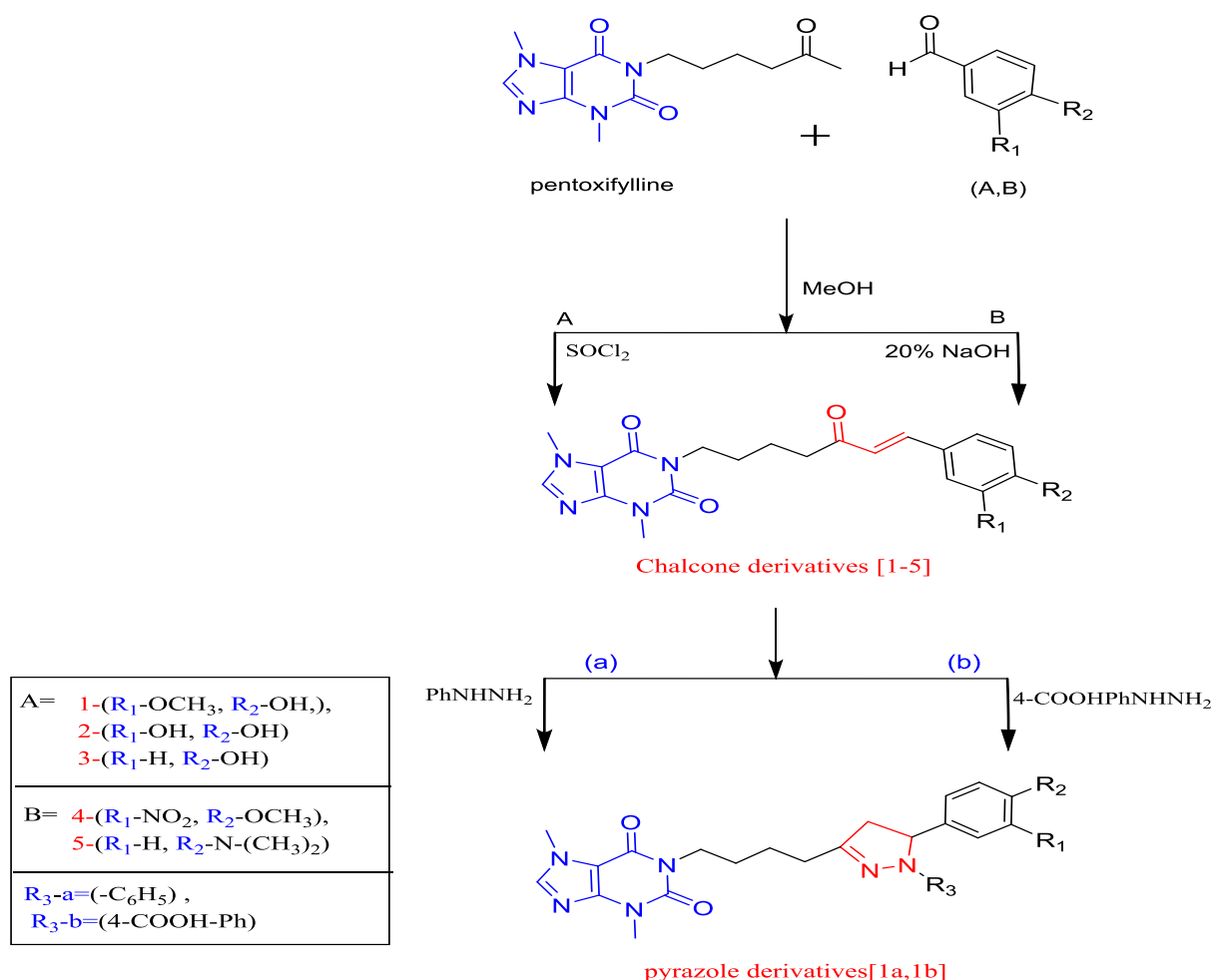


**Scheme (1) Synthesis of Intermediates and Target Compounds.**

**General procedures for the synthesis of chalcone derivatives:**

**Synthesis of chalcone derivatives [1-3]:**

Pentoxifylline (1 mmol) in methanol 15mL were mixed in a round bottom flask. Thionyl chloride 1 mL added dropwise for chalcones [1,2] and 0.5

mL for chalcone [3]. The solution was kept at room temperature for 20 min. Then (1 mmol) of suitable aldehyde derivatives 4-hydroxy-3-methoxybenzaldehyde [1], 3,4-dihydroxybenzaldehyde [2], 4-hydroxybenzaldehyde [3] in methanol (5ml)

added to the mixture. The resulting mixture stirred at room temperature for 2 hr., after completion of the reaction, standing overnight then poured into crushed ice. The colored precipitate obtained filtered, then recrystallized from dioxane: water. The resulting solid allowed to air dry[21,22].

### (E)-1-(7-(4-hydroxy-3-methoxyphenyl)-5-oxohept-6-en-1-yl)-3,7-dimethyl-3,7-dihydro-1H-purine-2,6-dione [1]:

Physical properties are revealed in Table (1). **Spectral data FT-IR using KBr disc** $\nu(cm^{-1})$: 3427(OH), 1699(C=O), 1654(C=O), 1595(C=N), 1458(C=C), 1234(C-O-CH$_3$). **$^1$H-NMR** (500MHz, DMSO-d$_6$), $\delta$, ppm: 3.39 (s,3H, NCH$_3$), 3.76 (s,3H, NCH$_3$), 3.93 (s,3H, N-CH$_3$), 6.54 (d, 1H,$\propto$HC=C), 6.79-7.27 (m, 3H, Ar-H), 7.45-7.49 (d, 1H,$\beta$HC=C), 9.07 (br.s, 1H, OH).

### (E)-1-(7-(3,4-dihydroxyphenyl)-5-oxohept-6-en-1-yl)-3,7-dimethyl-3,7-dihydro-1H-purine-2,6-dione [2]:

Physical properties are revealed in Table (1). **Spectral data FT-IR using KBr disc** $\nu(cm^{-1})$ 3390(OH), 1697(C=O), 1647(C=O), 1550(C=N) & (C=C).**$^1$H-NMR** (500MHz, DMSO-d$_6$), ($\delta$, ppm): 3.84 (s,6H, NCH$_3$), 6.53-7.44 (m, 3H, Ar-H), 8.14-8.21 (m, 2H,$\propto$,$\beta$HC=C), 9.46-9.56 (br.s, 2H, OH).

### (E)-1-(7-(4-hydroxyphenyl)-5-oxohept-6-en-1-yl)-3,7-dimethyl-3,7-dihydro-1H-purine-2,6-dione[3]:

Physical properties are revealed in Table (1). **Spectral data FT-IR using KBr disc** $\nu(cm^{-1})$: 3319(OH), 1691(C=O), 1654(C=O), 1602 &1554 (C=N) & (C=C).**$^1$H-NMR** (500MHz, DMSO-d$_6$), ($\delta$, ppm): 3.79-3.85 (s, 6H, NCH$_3$), 6.57-6.92 (m, 2H, Ar-H & 1H,$\propto$HC=C), 7.20-7.52 (m, 2H, Ar-H & 1H,$\beta$HC=C), 9.76 (br.s, 1H, OH).

### Synthesis of chalcone derivatives [4, 5]:

Pentoxifylline (1 mmol) in 15 mL methanol were mixed in a round bottom flask. Then, 2 mL of 20% aqueous sodium hydroxide [NaOH] solution added dropwise. Then (1 mmol) of suitable Aldehyde derivatives 4-methoxy-3-nitrobenzaldehyde [4], and 4-dimethylaminobenzaldehyde [5] in methanol (15 mL, 5ml) respectively, were added to the above mixture. The mixture stirred for 3hr. and 32hr. for chalcones [4, 5] respectively, at room temperature. Chalcone [5] Monitored by TLC, by using the mobile phase [chloroform: methanol (8:2)]. At the end of the reaction, poured into ice, the colored precipitate gained filtered then, recrystallized from dioxane: water. The resulting solid allowed to air dry[23].

### (E)-1-(7-(4-methoxy-3-nitrophenyl)-5-oxohept-6-en-1-yl)-3,7-dimethyl-3,7-dihydro-1H-purine-2,6-dione[4]:

Physical properties are revealed in Table (1). **Spectral data FT-IR using KBr disc** $\nu$ (cm$^{-1}$) 1701(C=O), 1658(C=O), 1612 & 1533 (C=N) & (C=C), 1236 (C-O-CH$_3$), 1356 & 1278 (NO$_2$). **$^1$H-NMR** (500MHz, DMSO-d$_6$), ($\delta$, ppm): 3.42 (s, 3H, NCH$_3$), 3.85 (s, 3H, NCH$_3$), 3.92 (s, 3H, OCH$_3$), 6.84-6.91(d, 1H,$\propto$HC=C), 7.38-7.40 (d, 1H, Ar-H), 7.56-7.60 (d, 1H, $\beta$HC=C), 7.93-8.00 (m, 1H, Ar-H), 8.24(m, 1H, Ar-H).

### (E)-1-(7-(4-(dimethylamino)phenyl)-5-oxohept-6-en-1-yl)-3,7-dimethyl-3,7-dihydro-1H-purine-2,6-dione[5]:

Physical properties are revealed in Table (1). **Spectral data FT-IR using KBr disc** $\nu$ (cm$^{-1}$) 1693(C=O), 1653(C=O), 1593 & 1529 (C=N) & (C=C), **$^1$H-NMR** (DMSO-d$_6$), ($\delta$, ppm): 2.96 (s,6H, N(CH$_3$)$_2$), 3.85 (s,6H, NCH$_3$), 6.59(d, 1H,$\propto$HC=C), 6.69-6.70 (d, 2H, Ar-H), 7.48 (d, 1H, $\beta$HC=C), 7.50-7.53 (d, 2H, Ar-H).

### General procedure for the synthesis of pyrazole derivatives:
### Synthesis of pyrazole derivatives [1a, 1b]:

A mixture of chalcone derivative [1] (0.25mmol) and phenylhydrazine (0.25 mmol) for pyrazole [1a] and 4-hydrazinobenzoic acid (0.25 mmol) for pyrazole [1b] in methanol 30 mL were mixed in a round bottom flask. Subsequently, 5 drops of glacial acetic acid were added dropwise. The obtained mixture was stirred for 1.5 hr. and 5 hr. for pyrazoles [1a, 1b], respectively at room temperature. At the end of the reaction, poured into ice, the colored precipitate attained filtered, then recrystallized from dioxane: water. The resulting solid allowed to air dry[24,25].

### 1-(4-(5-(4-hydroxy-3-methoxyphenyl)-1-phenyl-4,5-dihydro-1H-pyrazol-3-yl)butyl)-3,7-dimethyl-3,7-dihydro-1H-purine-2,6-dione[1a]:

Physical properties are revealed in Table (1). **Spectral data FT-IR using KBr disc** $\nu$ (cm$^{-1}$) 3454(OH), 1703(C=O), 1656 (C=O), 1604 (C=N), 1548(C=C). **$^1$H-NMR** (500MHz, DMSO-d$_6$) $\delta$, ppm: 3.05-3.10 (m, 2H, CH$_2$), 3.79-3.90 (br.s,9H, NCH$_3$), 5.93 (m, 1H, CH), 6.65-7.58 (m, 6H, Ar-H), 8.50-8.61(m, 2H, Ar-H), 9.01(br.s, 1H, OH).

### 4-(3-(4-(3,7-dimethyl-2,6-dioxo-2,3,6,7-tetrahydro-1H-purin-1-yl)butyl)-5-(4-hydroxy-3-methoxyphenyl)-4,5-dihydro-1H-pyrazol-1-yl)benzoic acid [1b]:

Physical properties are revealed in Table (1). Spectral data FT-IR using KBr disc $\nu$ (cm$^{-1}$)

3444(OH),1701 (C=O), 1654(C=O), 1606 (C=N), 1550(C=C). $^1$**H-NMR** (500MHz, DMSO-$d_6$), ($\delta$, ppm): 3.54 (m, 2H, $CH_2$), 3.75-3.82 (br.s,9H, $NCH_3$), 5.57 (m, 1H, CH), 6.74-7.27 (m, 3H, Ar-H), 7.58-7.77 (m, 2H, Ar-H), 8.61-8.75 (m, 2H, Ar-H), 9.64 (br.s, 1H, OH), 12.33 (br.s, 1H, OH).

**Table (1) The characterization data of the synthesized compounds**

| Compound | Chemical formula | M.Wt. | appearance | Yield (%) | Melting point (℃) | $R_f$ value |
|---|---|---|---|---|---|---|
| PTX | $C_{13}H_{18}N_4O_3$ | 278 | White powder | - | 104-107* | 0.48* |
| 1 | $C_{21}H_{24}N_4O_5$ | 412 | Green powder | 84 | 142-145 | 0.69 |
| 2 | $C_{20}H_{22}N_4O_5$ | 398 | Blue powder | 76 | 253-255(D) | 0.71 |
| 3 | $C_{20}H_{21}N_4O_4$ | 382 | yellow powder | 89 | 130-133 | 0.63 |
| 4 | $C_{21}H_{23}N_5O_6$ | 441 | Off-white powder | 95 | 189-190 | 0.71 |
| 5 | $C_{22}H_{27}N_5O_3$ | 409 | Yellow powder | 67 | 164-166 | 0.71 |
| 1a | $C_{27}H_{30}N_6O_4$ | 502 | Brown powder | 58 | 192-194 | 0.79 |
| 1b | $C_{28}H_{30}N_6O_6$ | 546 | Brown powder | 54 | 171-173 | 0.73 |

* Reported[26], D= decomposed.

## Computational methods
### ADME procedures
Pharmacokinetic or ADME (Absorption, Distribution, Metabolism, And Elimination) studies and other physicochemical properties of our designed compounds were determined by using the SwissADME server.

The chemical structure of newly designed compounds drawn by using chemAxon's Marvin JS then converted into SMILE name.

BIOLLED EGG is used to determine the lipophilicity and polarity of small molecules[27].

### The Docking Studies
The molecular docking studies are a valuable tool for the development of new compounds with the prediction of their affinity, interaction with receptors, and the most significantly the biological activity.

CCDC GOLD Suite (v. 5.7.1) include Hermes visualizer software (v. 1.10.1), used as assistance in the preparation of input files for docking with GOLD. Furthermore, visualize the receptors, ligands, type of interaction (H-bond, hydrophobic...etc.), active site, bond length calculation, pose prediction, and get images[28].

### Ligand and receptor preparation
Primarily, the chemical structure of our ligands was drawn by using ChemDraw professional (v.16.0) Software. Then, energy minimization for our compounds was done by using Chem3D (v.16.0) and by applying the MM2 force field.

Subsequently, the newly designed ligands were docked by using the 3D structure of the active target: the crystal structure of EGFR protein (PDB code: 4HJO) complexes with erlotinib, However, the receptor loaded into the Hermes module of GOLD from the protein data bank (PDB). Re-docking of the co-crystalized ligand was done to validate the docking process

Further, for precise ionization and tautomeric positions of amino acid residues, polar hydrogen atoms were added. Then, the structures of the EGFR kinase receptor protein are prepared by removing the crystallographic water molecules not involved in the active site. Also, the extraction of the original ligand from the receptor active site was done.

### Molecular docking protocol
Setup of the receptors for the docking process done by using Hermes visualizer software in the CCDC GOLD suite. Determination of the active site is according to the original ligand interaction site. The protein binding site with all the protein residues characterize within the (10 A°) of the standard ligand for the docking process.

All parameters used during the docking procedure chosen as default settings. The number of generated positions was set as (10), while the top-ranked solution was kept as default, also the early termination choice was turned off. Chemscore kinase is used as a configuration template. While the piecewise linear potential (ChemPLP) is used as a scoring function.

Finally, the results were saved as mol.2 files. That provides information about the best binding manner, the free energy of binding, and docked poses. These results were studied precisely to define the best binding and interaction of our designed ligand with amino acid residues of the EGFR receptor.

### Preliminary cytotoxicity studies
The preliminary anticancer activity was done at the University of Mustansiriyah/college of pharmacy. This test was performed using the MTT

colorimetric assay[29]. The methodology described here is to examine the cytotoxicity effects of synthesized compounds [1, 2, 3, 4, 5, 1a, 1b], on human A549 (lung) cancer cell line.

## MTT colorimetric assay

The MTT colorimetric assay was used to estimate the effects of synthesized compounds [1, 2, 3, 4, 5, 1a, 1b] on lung cancer cell viability. Cells suspension (100 $\mu$l) were added into 96-well flat-bottom tissue culture plated at concentrations of (5 x $10^3$ cells per well) and incubated for (24hr.) in standard conditions, (4 x $10^3$ cells per well) for 48hr, and (3 x $10^3$ cells per well) for 72hr. incubation. Afterward, 24hr completed the cells were treated with 50 $\mu$M from each compound. When a recovery period of 24hr, 48hr, and 72hr, completed the cell culture medium was removed and cultures were incubated for 4hr at 37 C$^\circ$ with a medium containing 30 $\mu$l of MTT solution (3mg/ml of MTT powder in PBS). Only 100 $\mu$l of growth media were added to control wells. Then, DMSO 100 $\mu$l was added to each well then, kept at room temperature in the dark condition for about (15-20 min)[30]. The assay was done in a triplicate and the optical density of each plate (well) was measured at a transmitting wavelength (520-600 nm) by using Multiscan Reader. The inhibition rate of cell growth (percentage of cytotoxicity) was calculated as follows:
[Inhibition Rate percentage= (A-B/A)*100].

## Statistical analysis

All statistical analyses of MTT assay and $IC_{50}$ data of tested compounds [1, 2, 3, 4, 5, 1a, 1b] on A549 cells were done by using the nonlinear curve fitting software prism pad software. Comparison between all groups within the same plate of MTT was evaluated by one-way ANOVA with Tukey (prism and software). Values of $p > 0.05$ were considered statistically significant.

## RESULTS AND DISCUSSION
### Chemistry

In the first step of the reaction, we synthesize chalcone derivatives [1-5] with the Claisen-Schmidt condensation reaction. Subsequently, in the second step, the target compounds pyrazoles [1a, 1b]. The first three chalcones [1, 2, 3] that contain a hydroxyl group scheme (1) not achieved via conventional base-catalyst reactions.

Chalcones [1, 2, 3] were synthesized by using Thionyl chloride (SOCl$_2$) as a novel acid catalyst. This catalyst is used with aromatic aldehydes or ketones containing hydroxyl groups to prevent the formation of salt. As well as, decrease the activity of aldehyde substituents due to delocalization of the anion[31] in the presence of base-catalyst with the common synthetic procedures. Moreover, this method is considered simple, convenient, avoid using of protecting group, and HCl formed in situ instead of using it as a gas[21,22]. The reaction of pyrazoline synthesis catalyzed by acid (glacial acetic acid), in presence of hydrazine derivatives (phenylhydrazine, and 4-hydrazinobenzoic acid) [32].

## ADME results interpretation

SwissADME server[27] was used for in silico prediction of the physicochemical and ADME properties of designed compounds. It is a supportive and inexpensive method to detect the ADME properties before synthesis and biological testing and to exclude ligands inadequate with an unacceptable pharmacokinetic profile[33,34].

These parameters include the topological polar surface area (TPSA), used to describe the ability of drugs to permeate cells, compounds with TPSA<140Å$^2$ that mean high permeability and bioavailability[35]. Our results showed that all compounds have TPSA <140Å2 range from (82.13-138.58). However, all the ligands expected passively and highly absorb from The GIT.

Another useful molecular descriptor is Lipinski's "rule of five" (RO5) briefly states that compounds should have a molecular mass of ≤ 500 Daltons, ≤5 H-bond donor, ≤10 H-bond acceptor, log p ≤5 (octanol-water partition coefficient) to be absorbed orally otherwise will have poor bioavailability and permeability [36]. Our results showed that all synthesized compounds satisfy the RO5 except compound [1b], which does not satisfied RO5 due to M.Wt. >500, and the number of nitrogen\oxygen atoms more than 10 as shown in Table (2). According to Bartzatt[37] reported that among 16 effective anticancer drugs used in the treatment of lung cancer seven drugs have more than one violation in RO5, Such as docetaxel, etoposide, and pemetrexed. Additionally, the bioavailability score of ligands was 0.55 except 1b 0.56.

**Table 2. ADME results of intermediates and target compounds.**

| Comp. | H-donor | H-acceptor | MR | TPSA | GI Abs. | BBB permeability | Bio-availability | Lipinski violation |
|-------|---------|------------|--------|--------|------|------------------|------------------|--------------------|
| 1 | 1 | 6 | 114.40 | 108.35 | High | No | 0.55 | 0 |
| 2 | 2 | 6 | 109.93 | 119.35 | High | No | 0.55 | 0 |

| 3 | 1 | 5 | 107.91 | 99.12 | High | No | 0.55 | 0 |
|---|---|---|--------|-------|------|-----|------|---|
| 4 | 0 | 7 | 121.20 | 133.94 | High | No | 0.55 | 1 [N or O > 10] |
| 5 | 0 | 4 | 120.09 | 82.13 | High | No | 0.55 | 0 |
| 1a | 1 | 6 | 150.64 | 106.88 | High | No | 0.55 | 1[M.WT.> 500] |
| 1b | 2 | 8 | 170.13 | 138.58 | High | No | 0.56 | 2 [N or O >10, and M.WT.>500]] |

### Interpretation of docking results

GOLD is a "genetic algorithm for docking flexible ligands into protein binding sites" [38]. Generally, GOLD has the advantage to predict the pose and gives perfect outcomes for virtual screening[39]. It is supplied as one part of the GOLD suite, which includes extra softwares such as Hermes, CSD python, mercury, ConQuest, mogul, and others.

Energy optimization methods were used to locate stable and minimum energy conformation by changing the geometry of the structure.

The docking studies result in the prediction of binding energies and selectivity for the designed compounds to protein (EGFR) through studying the molecular contact among the active binding sites of the protein, and designed compounds.

The EGFR inhibitory activities of designed compounds, and erlotinib, were rated depending on their PLP fitnes. Table (3) shown The PLP fitness of the docked compounds on EGFR protein.

GOLD software also gives the distance of hydrogen bonding between our designed ligands and a specific protein as well as all bonds length was $\leq 3A^{o[40]}$.

Docking results showing that all the designed compounds exhibit better binding energies with receptor active pocket and expected promising activity with EGFR protein since it binds to the amino acids (AAs) residue of the active site through H-bonds along with hydrophobic interaction and other short contacts.

However, compounds [3, and 1a] with EGFR protein show the highest PLP fitness value (90.78, 91.04) respectively, and H-bonding with AAs as represented in Table (3)

All other ligands exhibit less binding energies than the standard drug Erlotinib that give PLP fitness value (89.92) and it is N-1 atom form H-bond with MTE769, (O-CH$_3$) group with LYS704 and N-3 atom form H-bond through H$_2$O Bridge with THR766 and THR830 AAs along with hydrophobic interactions as depicted in Figure (1).

As illustrated in figure (2) compound [4] forms H-bond via C=O of the xanthine ring with THR830 along with other short contacts that reinforce the binding and give PLP value (87.06). The best pose of compound [5] that give PLP fitness value (85.72) form H-bond through C=O group of α,β-unsaturated system with the LYS721 AAs along with short contact as shown in Figure (3). We should notice that compound [5] exhibits potent inhibitory activity in cytotoxicity (In Vitro) study this may be due to the bond has higher stability than other derivatives. On the other hand, the PLP value for compound [1b] was (88.55) and give H-bond with MTE769 AAs.

**Table (3) The Binding Energies for Pentoxifylline Derivatives and standard TKIs erlotinib Docked With EGFR**

| Comp. | EGFR binding energy (PLP fitness) | Amino acid included in H-bonding | Amino acid included in short contacts |
|-------|-----------------------------------|----------------------------------|---------------------------------------|
| 1 | 86.82 | ALA719, ASP831, LEU764 | ALA719, LEU694, VAL702, MTE769 |
| 2 | 88.52 | PHE832 | LEU694,,LEU820, PHE832, LEU764, THR830, VAL702, LYS721 |
| 3 | 91.04 | PHE832 | VAL702, PHE832, MTE769, ALA719, LEU694,,LEU820, LYS721 |
| 4 | 87.06 | THR830 | LEU694, LYS721, THR830, LEU764,CYS751, ASP831,MET742 |
| 5 | 85.72 | LYS721 | VAL702, LYS721, THR830 through H$_2$O bridge with THR766, LEU764,LEU753,PHE832,MET742 |

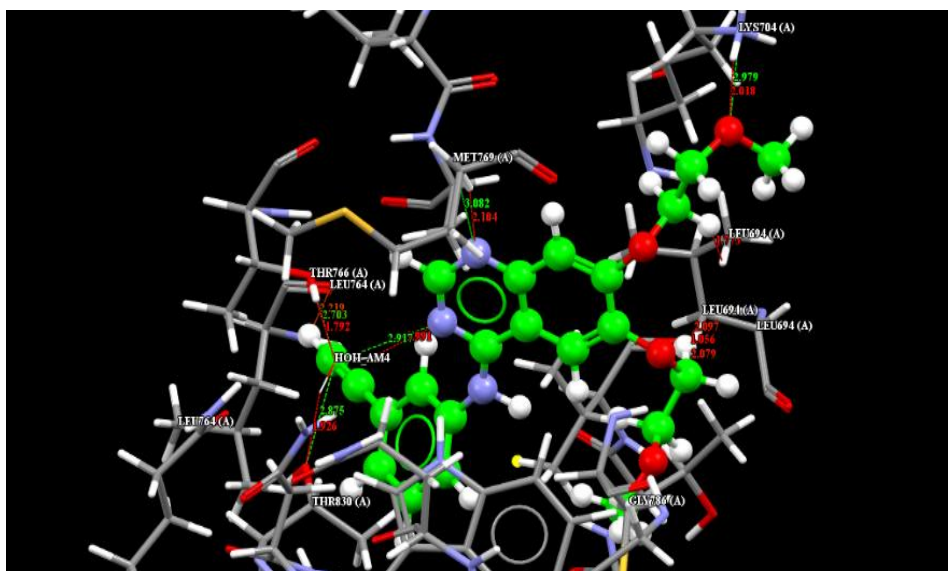| 1a | 90.78 | LYS721(2)*, LEU764, ALA698 | VAL702, PHE699, ALA719, LEU694,LEU764, LYS721, THR830 through H₂O bridge with THR766, |
|---|---|---|---|
| 1b | 88.55 | MTE769 | PRO717,MET769, VAL702, LYS721, GLY697,PHE699, ARG817, THR830 |
| Erlotinib | 89.92 | MTE769, LYS704, THR830 through H₂O bridge with THR766 | LEU694,LYS704, MTE769,LEU764 ,THR830 through H₂O bridge with THR766, |

*Number in brackets refer to no. of H-bonds.



**Fig.(1):H-bond and short contact interaction profile for the standard drug Erlotinib binding with EGFR receptor (PDB code: 4HJO). The interaction between erlotinib and amino acid residues by H-bond [MTE769, LYS704, and THR830 through H2O Bridge with THR766] represents in green while for short contact in red. [Erlotinib: ball and stick style, while amino acids in capped sticks].**
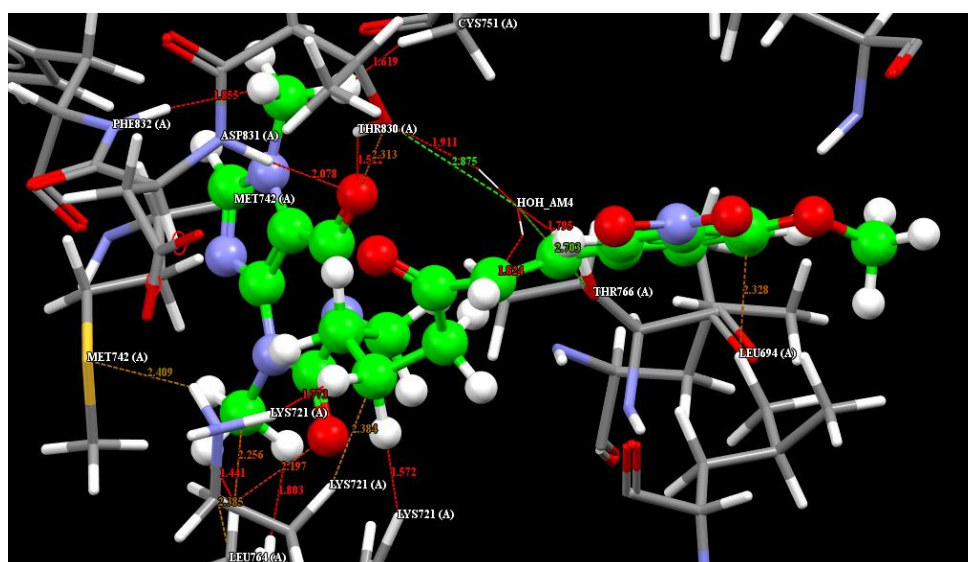


**Fig.(2):H-bond and short contact interaction profile for compound [4] binding with EGFR receptor (PDB code: 4HJO). The interaction between compound [4] and amino acid residues by H-bond [THR830] represents in green while for short contact in red. [Erlotinib: ball and stick style, while amino acids in capped sticks].**
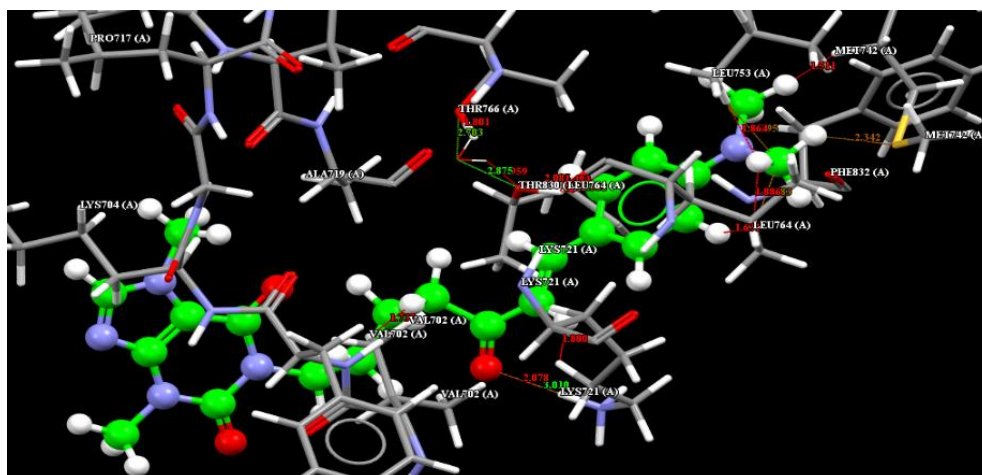
**Fig.(3): H-bond and short contact interaction profile for compound [5] binding with EGFR receptor (PDB code: 4HJO). The interaction between compound [5] and amino acid residues by H-bond [LYS721] represents in green while for short contact in red. [Erlotinib: ball and stick style, while amino acids in capped sticks].**

### Results of cytotoxicity studies

The achieved data exposed that the synthesized compounds [3, 4, 5, 1b] showed promising antitumor activity. From the tested compounds, the best and more potent cytotoxic effect was for compound [5] with an $IC_{50}$ value of 11.44 $\mu M$, considered as twofold more active than erlotinib with an $IC_{50}$ value of 25.23 $\mu M$ and this means lower concentration by half from compound [5] needed to inhibit cancerous A549 cell growth in comparison to standard. Meanwhile, compounds [4, 1b] exhibit significantly higher $IC_{50}$ values (22.98, and 24) $\mu M$, respectively. Lastly, Compound [3] shows a significantly lower $IC_{50}$ value of 29.3 $\mu M$ than the standard. Table (4) summarized $IC_{50}$ values for A549 cell line when treated for 72hr with compounds [3, 4, 5, 1b] with diverse concentrations (100, 50, 25, 12.5, 6.25, 3.125, 1.562, 0.781, 0.390, and, 0.195 $\mu M$) by using MTT assay. Figure (4) represent dose response curves of $IC_{50}$ values.

**Table (4) Cytotoxicity of the tested compounds [3, 4, 5, 1b] and erlotinib as standard against A549 (lung) cancer cell line**

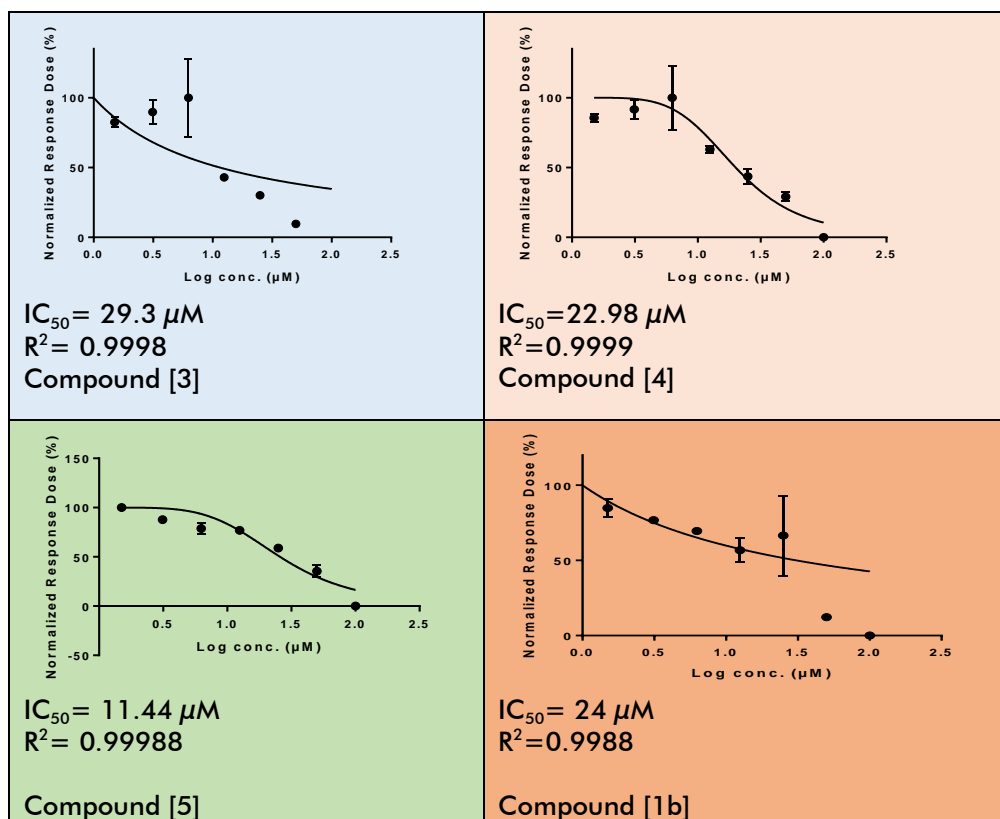| Comp. | $IC_{50}$ ($\mu M$) |
|---|---|
| 3 | 29.3 |
| 4 | 22.98 |
| 5 | 11.44 |
| 1b | 24 |
| Erlotinib | 25.23 |

**Fig.(4):Dose-response curves of IC$_{50}$ for A549 for compounds [3, 4, 5, 1b], treated for 72hr. with different ranges of concentrations (100, 50, 25, 12.5, 6.25, 3.125, 1.562, 0.781, 0.390, and, 0.195 μM). The normalized dose-response was plotted with log concentrations of compounds [3, 4, 5, 1b]. The determination of IC$_{50}$ values was done using nonlinear regression analysis (prism). The standard error of the mean percent (SEM) represented by Error bars for triplicate analysis.**

The results revealed that: the % of cell death is time-dependent increased with time from 24hr. to 72hr. As shown in Figure (5) all the tested compounds show considerable variation in responsiveness to cell death compared to standard. The synthesized compounds exhibit significantly lower percentage of cell death than erlotinib (82.40%) on the other hand compound [5] was very close and slightly lower than erlotinib with 81.21% of cell death. while compounds [3, 4, 1b] demonstrate a moderate percentage of cell death. Further, compounds [1, 2, 1a] show the lowest percentage ranges from (38.51%-44.63%).
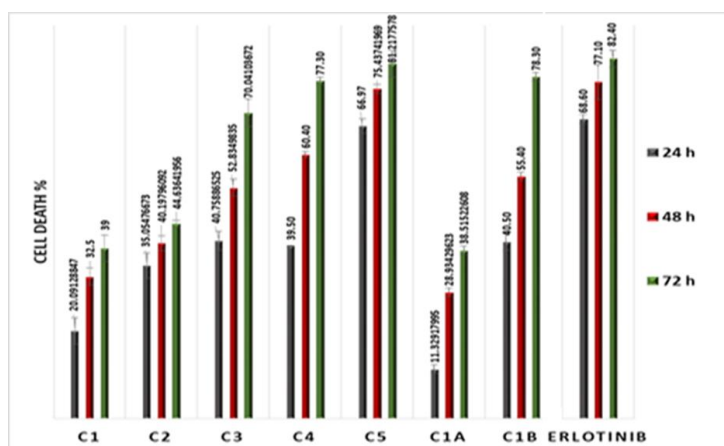


**Fig.(5):In vitro assessment of % cell death of the Human lung cell line (A549) was evaluated by using MTT assay by using a 96-well plate after 24hr, 48, 72hr. Treated with 50μM of compounds [1, 2, 3, 4, 5, 1a, 1b]. Data are shown as % mean± SEM of cell death for 3 separate experiments.**

## CONCLUSION

In conclusion, a new series of chalcone, and pyrazole derivatives [1, 2, 3, 4, 5, 1a, 1b] were synthesized from pentoxifylline successfully. Besides, their structures were identified through different spectral data including FT-IR, and $^1$H-NMR. Evaluation of anticancer activity against the A549 (lung) cancer cell line was done. Among the tested compounds, the most promising was compound [5] with an $IC_{50}$ value of 11.44 $\mu M$ considered as two times more active than the positive control erlotinib with an $IC_{50}$ value of 25.23 $\mu M$. Besides, kill A549 cancerous cells by (81.21%) considered slightly lower than erlotinib with 82.40% of cell death. In Silico experiments, including ADME studies exhibited that all designed compounds appear passively and highly absorbed from The GIT. Also, all compounds satisfied the RO5 except compounds [1b]. The docking studies showed excellent correlation with in vitro results for ligands selectivity towards EGFR protein.

### Acknowledgment

### Conflict of interests
The authors declared no conflict of interest.

## REFERENCES

1. Monteiro JP, Alves MG, Oliveira PF, Silva BM. Structure-bioactivity relationships of methylxanthines: Trying to make sense of all the promises and the drawbacks. Molecules. 2016;21(8).
2. Singh N, Shreshtha AK, Thakur MS, Patra S. Xanthine scaffold: scope and potential in drug development. Heliyon. 2018;4(10):e00829.
3. Kavi KPB, Bandopadhyay R, Suravajhala P. Xanthine Derivatives: A Molecular Modeling Perspective. In: Agricultural Bioinformatics. 2014. p. 283–91.
4. Abdel-Salam OME, Baiuomy AR, El-Shenawy SM, Arbid MS. The anti-inflammatory effects of the phosphodiesterase inhibitor pentoxifylline in the rat. Pharmacol Res. 2003;47(4):331–40.
5. Donate-Correa J, Tagua VG, Ferri C, Martín-Núñez E, Hernández-Carballo C, Ureña-Torres P, et al. Pentoxifylline for Renal Protection in Diabetic Kidney Disease. A Model of Old Drugs for New Horizons. J Clin Med. 2019;8(3):287.
6. ABK Bogucka-Kocka A, Och AA, Och MM, Kocki JJ. Pentoxifylline-rescue for the oncological patient. Anticancer and protective properties of an alkaloid derivative. 2012;(081).
7. Abou-Zied HA, Youssif BGM, Mohamed MFA, Hayallah AM, Abdel-Aziz M. EGFR inhibitors and apoptotic inducers: Design, synthesis, anticancer activity and docking studies of novel xanthine derivatives carrying chalcone moiety as hybrid molecules. Bioorg Chem. 2019;89(March):102997.
8. Barancik M, Bohacova V, Gibalova L, Sedlak J, Sulova Z, Breier A. Potentiation of anticancer drugs: Effects of pentoxifylline on neoplastic cells. Int J Mol Sci. 2012;13(1):369–82.
9. Rammohan A, Reddy JS, Sravya G, Rao CN, Zyryanov G V. Chalcone synthesis, properties, and medicinal applications: a review. Environ Chem Lett. 2020;18(2):433–58.
10. Gaonkar SL, Vignesh UN. Synthesis and pharmacological properties of chalcones: a review. Res Chem Intermed. 2017;43(11):6043–77.
11. Kalirajan R, Sivakumar SU, Jubie S, Gowramma B, Suresh B. Synthesis and biological evaluation of some heterocyclic derivatives of Chalcones. Int J ChemTech Res. 2009;1(1):27–34.
12. Syam S, Abdelwahab SI, Al-Mamary MA, Mohan S. Synthesis of chalcones with anticancer activities. Molecules. 2012;17(6):6179–95.
13. Wang YJ, Zhou DG, He FC, Chen JX, Chen YZ, Gan XH, et al. Synthesis and antiviral bioactivity of novel chalcone derivatives containing purine moiety. Chinese Chem Lett. 2018;29(1):127–30.
14. Jyoti, Gaur R, Kumar Y, Cheema HS, Kapkoti DS, Darokar MP, et al. Synthesis, molecular modelling studies of indolyl chalcone derivatives and their antimalarial activity evaluation. Nat Prod Res. 2019;0(0):1–8.
15. Sharshira EM, Mahrous Hamada NM. Synthesis and in vitro antimicrobial activity of some pyrazolyl-1- carboxamide derivatives. Molecules. 2011;16(9):7736–45.
16. Bennani FE, Doudach L, Cherrah Y, Ramli Y, Karrouchi K, Ansar M, et al. Overview of recent developments of pyrazole derivatives as an anticancer agent in different cell line. Vol. 97, Bioorganic Chemistry. Elsevier Inc.; 2020.
17. Qiu KM, Wang HH, Wang LM, Luo Y, Yang XH, Wang XM, et al. Design, synthesis and biological evaluation of pyrazolyl-thiazolinone derivatives as potential EGFR and HER-2 kinase inhibitors. Bioorganic Med Chem. 2012;20(6):2010–8.
18. Zeng H, Zhang H. Combined 3D-QSAR

modeling and molecular docking study on 1,4-dihydroindeno[1,2-c]pyrazoles as VEGFR-2 kinase inhibitors. J Mol Graph Model. 2010;29(1):54–71.

19. Ferguson FM, Doctor ZM, Ficarro SB, Marto JA, Kim ND, Sim T, et al. Synthesis and structure activity relationships of a series of 4-amino-1H-pyrazoles as covalent inhibitors of CDK14. Bioorganic Med Chem Lett. 2019;29(15):1985–93.

20. Kamal A, Shaik AB, Jain N, Kishor C, Nagabhushana A, Supriya B, et al. Design and synthesis of pyrazole-oxindole conjugates targeting tubulin polymerization as new anticancer agents. Eur J Med Chem. 2015;92:501–13.

21. Hou YX, Sun SW, Liu Y, Li Y, Liu XH, Wang W, et al. An improved method for the synthesis of butein using SOCl2/ETOH as catalyst and deciphering its inhibition mechanism on xanthine oxidase. Molecules. 2019;24(10).

22. Hu Z, Liu J, Dong Z, Guo L, Wang D, Zeng P. Synthesis of chalcones catalysed by SOCl2/EtOH. J Chem Res. 2004;(2):158–9.

23. Danao K, Mahajan U. Mini review : Chalcone derivatives as Antimalarial agent. Int J Pharm Chem. 2018;08(08):45–52.

24. Insuasty B, Ramírez J, Becerra D, Echeverry C, Quiroga J, Abonia R, et al. An efficient synthesis of new caffeine-based chalcones, pyrazolines and pyrazolo[3,4-b][1,4]diazepines as potential antimalarial, antitrypanosomal and antileishmanial agents. Eur J Med Chem. 2015;93:401–13.

25. Rostom SAF, Badr MH, Abd El Razik HA, Ashour HMA, Abdel Wahab AE. Synthesis of some pyrazolines and pyrimidines derived from polymethoxy chalcones as anticancer and antimicrobial agents. Arch Pharm (Weinheim). 2011;344(9):572–87.

26. Lianawati T, Wahyuningsih I, Aditama L, Brittain HG. pentoxifylline. Acad Press Inc. 1998;25(1).

27. Daina A, Michielin O, Zoete V. SwissADME: A free web tool to evaluate pharmacokinetics, drug-likeness and medicinal chemistry friendliness of small molecules. Vol. 7, Scientific Reports. Nature Publishing Group; 2017.

28. Nawaz F, Alam O, Perwez A, Rizvi MA, Naim MJ, Siddiqui N, et al. 3′-(4-(Benzyloxy)phenyl)-1′-phenyl-5-(heteroaryl/aryl)-3,4-dihydro-1′H,2H-[3,4′-bipyrazole]-2-carboxamides as EGFR kinase inhibitors: Synthesis, anticancer evaluation, and molecular docking studies. Arch Pharm (Weinheim). 2020;353(4):1–18.

29. Mohammed AW, Arif IS, Jasim GA. The Cytotoxic Effect of Metformin on RD Cell Line. Al Mustansiriyah J Pharm Sci. 2019;19(1):85–94.

30. Chang J, Ren H, Zhao M, Chong Y, Zhao W, He Y, et al. Development of a series of novel 4-anlinoquinazoline derivatives possessing quinazoline skeleton: Design, synthesis, EGFR kinase inhibitory efficacy, and evaluation of anticancer activities in vitro. Eur J Med Chem. 2017;138:669–88.

31. Jayapal MR, Sreedhar NY. Synthesis of 2,6-dihydroxy substituted chalcones by aldol condensation using SOCL2/ETOH. Int J Pharm Pharm Sci. 2011;3(1):127–9.

32. Thirunarayanan G, Sekar KG. Solvent-free one-pot cyclization and acetylation of chalcones: Synthesis of some 1-acetyl pyrazoles and spectral correlations of 1-(3-(3,4-dimethylphenyl)-5-(substituted phenyl)-4,5-dihydro-1H-pyrazole-1-yl) ethanones. J Saudi Chem Soc. 2016;20(6):661–72.

33. Hou T, Wang J, Zhang W, Xu X. ADME evaluation in drug discovery. 7. prediction of oral absorption by correlation and classification. J Chem Inf Model. 2007;47(1):208–18.

34. Abdul Muhaimen Amjed Adnan, Monther Faisal Mahdi A kareem K. Design, Synthesis, and Acute Anti-inflammatory Assessment of New 2-methyl Benzoimidazole Derivatives Having 4-Thiazolidinone Nucleus. Al Mustansiriyah J Pharm Sci. 2019;19(4):151–60.

35. Pajouhesh H, Lenz GR. Medicinal chemical properties of successful central nervous system drugs. J Am Soc Exp Neurother. 2005;2(4):541–53.

36. john M.beale J john HB. Wilson and Gisvold's textbook oforganic medicinal and pharmaceutical chemistry [Internet]. 12th ed. ohn M.beale J john HB, editor. Lippincott Williams & Wilkins, a Wolters Kluwer business. First; 2004. 1–1022 p.

37. Bartzatt R. Pharmaceutical properties and drug likeness of anticancer drugs administered for the clinical treatment of lung cancer. Int J Cancer Res Prev. 2016;9(3):279–95.

38. Gareth Jones1 *, Peter Willett1, Robert C. Glen2 ARL and RT. Development and Validation of a Genetic Algorithm for Flexible Docking Gareth. J Mol Biol. 1997;267:727–48.

39. Verdonk ML, Cole JC, Hartshorn MJ, Murray CW, Taylor RD. Improved protein–ligand docking using GOLD. Proteins. 2003;52(January):609–23.

40. Alvarez J, Shoichet B. Virtual screening in drug discovery. Virtual Screening in Drug Discovery. 2005. 1–470 p.